

# SCIENTIFIC REPORTS

OPEN

## Chaoticons described by nonlocal nonlinear Schrödinger equation

Lanhua Zhong<sup>1,2</sup>, Yuqi Li<sup>3</sup>, Yong Chen<sup>3</sup>, Weiyi Hong<sup>1</sup>, Wei Hu<sup>1</sup> & Qi Guo<sup>1</sup>

Received: 26 September 2016

Accepted: 20 December 2016

Published: 30 January 2017

It is shown that the unstable evolutions of the Hermite-Gauss-type stationary solutions for the nonlocal nonlinear Schrödinger equation with the exponential-decay response function can evolve into chaotic states. This new kind of entities are referred to as chaoticons because they exhibit not only chaotic properties (with positive Lyapunov exponents and spatial decoherence) but also soliton-like properties (with invariant statistic width and interaction of quasi-elastic collisions).

Solitons are self-reinforcing stable localized wave entities that maintain their shapes when they evolve in nonlinear systems, and are caused by a balance between nonlinearity and dispersion in the systems. They have been demonstrated in a large variety of physical systems, including optics, hydrodynamics, particle physics, electrical circuits and even astrophysics<sup>1-3</sup>. Over the past three decades, optical solitons<sup>4-11</sup> have been at the forefront of soliton research, which are modelled by the nonlinear Schrödinger equation  $i\partial q/\partial t + (1/2)\partial^2 q/\partial x^2 + |q|^2 q = 0$  (for the local nonlinearity)<sup>4-6</sup> and its generalized form, the nonlocal nonlinear Schrödinger equation (NNLSE) (for the nonlocal nonlinearity)<sup>10-29</sup>. The (1 + 1)-dimensional form of the NNLSE is<sup>11-13</sup>

$$i\frac{\partial q(x, t)}{\partial t} + \frac{1}{2}\frac{\partial^2 q(x, t)}{\partial x^2} + q(x, t) \int_{-\infty}^{\infty} R(x - \xi) |q(\xi, t)|^2 d\xi = 0, \quad (1)$$

where the real positive function  $R(x)$  is the (nonlinear) response function, which must be symmetry for the existence of the soliton-like solutions<sup>30</sup>. The Hamiltonian of Eq. (1)  $H = \int_{-\infty}^{\infty} [|\partial q(x)/\partial x|^2 - \int_{-\infty}^{\infty} R(x - \xi) |q(\xi)|^2 d\xi] dx$  is conserved<sup>29</sup>.

The nonlocal nonlinearity (the convolution integral) in Eq. (1) means that the wave-induced “potential” at a certain spatial point  $x$ ,  $V(x, t) = -\int_{-\infty}^{\infty} R(x - \xi) |q(\xi, t)|^2 d\xi$ , is determined not only by the wave  $q(x, t)$  at that point but also by the wave in its vicinity. This kind of nonlocal nonlinear response has been found in several systems, such as Bose-Einstein condensates<sup>31,32</sup>, atomic vapors<sup>33</sup>, nematic liquid crystals<sup>15,16</sup>, thermal susceptibilities<sup>34</sup>, etc. The stronger the nonlocality, the more extended the wave distribution contributing to the “potential”  $V$ <sup>13,14,35</sup>. Different from the (local) nonlinear Schrödinger equation [when  $R(x) = \delta(x)$  in Eq. (1)], nonlocality has profound effects on the dynamics of solitons. For example, the interaction of two nonlocal solitons can have both a long-range mode<sup>22,23,35</sup> and a short-range mode<sup>24,25,35</sup>, but two local solitons interact with each other only in a short-range one<sup>7,35</sup>; and the NNLSE [Eq. (1)] can support the multi-hump solitons with the Hermite-Gauss-type (HGT) profiles<sup>18-21</sup>, but the nonlinear Schrödinger equation admits only the single-hump solitons<sup>5</sup>. However, the NNLSE may not guarantee the existence of all high order HGT-solitons. The response function also plays an important role. The NNLSE with the Gaussian response function can support the HGT-solitons without upper threshold of the hump-number<sup>18-20</sup>. Contrastively, the NNLSE with the exponential-decay response function<sup>13</sup> only admits of the HGT-solitons with the hump-number less than five<sup>20</sup>. The crucial difference between such two kinds of response functions is<sup>11,35</sup> that the former is non-singular and the potential  $V$  can be simplified to a quadratic form in the limit of strong nonlocality, while the latter that can describe physically real materials is singular and the corresponding NNLSE cannot be generally reduced to a linear Snyder-Mitchell mode<sup>12</sup>.

Unlike the (local) nonlinear Schrödinger equation, which is integrable and can be solved via the inverse scattering transform method<sup>1-3</sup>, the NNLSE given by Eq. (1) is non-integrable<sup>9,29</sup> and cannot be solved analytically. In a non-integrable nonlinear system, chaos often appears. Chaos is generally agreed to denote the aperiodic long-term behavior of a bounded deterministic system that exhibits sensitive dependence on initial conditions.

<sup>1</sup>Guangdong Provincial Key Laboratory of Nanophotonic Functional Materials and Devices, South China Normal University, Guangzhou 510631, P.R. China. <sup>2</sup>Physical Science and Technology School, Lingnan Normal University, Zhanjiang 524048, P.R. China. <sup>3</sup>Shanghai Key Laboratory of Trustworthy Computing, East China Normal University, Shanghai 200062, P.R. China. Correspondence and requests for materials should be addressed to Q.G. (email: guoq@scnu.edu.cn)

And the most common criterion for chaos is a positive Lyapunov exponent, which means that two initially arbitrarily close trajectories in phase space diverge exponentially in time<sup>36–38</sup>.

In this letter, we investigate the evolution of the (1 + 1)-dimensional NNLSE with the exponential-decay response function for the initial inputs of the HGT stationary solutions. As has been mentioned<sup>20</sup>, the HGT stationary solutions with the hump-number more than 4 always evolve unstably. We, however, find that such an unstable evolution of every HGT stationary solution can develop into a chaotic state, which is characterized by the positive Lyapunov exponent and spatial decoherence. Moreover, it also exhibits the soliton-like properties: the invariant statistic width during the evolution and the quasi-elastic collisions during the interaction. Therefore, we refer to these entities as chaoticons, as they are termed for the spatiotemporal chaotic localized states in the dissipative systems<sup>39,40</sup>. We believe it is the first time, to the best of our knowledge, to present the solutions in the conservative system (Hamiltonian system<sup>36</sup>) described by the NNLSE which possess both the chaotic and soliton-like properties.

### Unstable evolution of HGT stationary solutions

We consider here the NNLSE [Eq. (1)] with the exponential-decay response function<sup>13,20,22</sup>

$$R(x) = \frac{1}{2w_m} \exp\left(-\frac{|x|}{w_m}\right), \quad (2)$$

which has a singularity at  $x=0$ . This case corresponds to the model for the propagation of the (1 + 1)-dimensional paraxial optical beam in nematic liquid crystals, which can be described by the coupled partial differential equations<sup>10,11,15,16</sup>

$$\begin{aligned} i\frac{\partial q}{\partial t} + \frac{1}{2}\frac{\partial^2 q}{\partial x^2} - qV &= 0, \\ V - w_m^2\frac{\partial^2 V}{\partial x^2} + |q|^2 &= 0, \end{aligned} \quad (3)$$

where  $q$  is the dimensionless slowly-varying complex amplitude of the optical field,  $x$  and “time”  $t$  stand for, respectively, the dimensionless transverse coordinate and the dimensionless propagation direction coordinate, the “potential”  $-V$  represents the nonlinear induced refractive index. Obviously, the set of equations (3) is equivalent to Eqs. (1) and (2). The relative scale of the characteristic length of the response function  $w_m$  to the statistic width of the wave  $w$  denotes the degree of nonlocality<sup>13,14</sup>, where  $w$  is defined by the second-order moment  $w(t) = \left\{2 \int_{-\infty}^{\infty} [x - x_c(t)]^2 |q(x, t)|^2 dx/P\right\}^{1/2}$  [ $x_c(t) = \int_{-\infty}^{\infty} x |q(x, t)|^2 dx/P$  is the center of the wave and  $P = \int_{-\infty}^{\infty} |q(x, t)|^2 dx$  is the power that is conserved]. The larger the ratio  $w_m/w$ , the stronger the nonlocality.

The NNLSE [Eq. (1)] permits the stationary solutions of the form<sup>19–21</sup>

$$q(x, t) = u_N(x) \exp(ib_N t), \quad (4)$$

where  $u_N$  is a real function and  $b_N$  is a real constant. It was numerically found that in the case with the exponential-decay response function  $u_N(x)$  is of  $N$ -humps ( $N=1, 2, 3, \dots$ ) HGT-structure<sup>20,41</sup>, specially,  $u_1(x)$  has a single-hump Gauss-type shape. It was also proved that  $u_N(x)$  ( $N \geq 2$ ) can exist only when the parameters  $w_m$  and  $b_N$  satisfy  $w_m > 1/\sqrt{2b_N}$ <sup>22,42</sup>.

We simulate Eqs. (1) and (2) with the initial inputs of the HGT stationary solutions  $q(x, 0) = u_N(x)$  by means of the split-step method<sup>43</sup>. The case of strongly nonlocal nonlinearity [ $w_m = 10$  and  $w(0) = 1$  unless otherwise stated] is considered. The unstable evolution<sup>41</sup> of the HGT stationary solutions ( $N > 4$ ) are given in Fig. 1, where only solutions with  $N=7$  and 12 are displayed without loss of generality. It is clear that the profiles starting from regular multi-humps turn to be irregular shapes, several of which are shown in Fig. 1(e). The evolution diagrams remind us the behavior of chaos.

### Chaotic behavior: positive Lyapunov exponents

Since a positive Lyapunov exponent is a signature of chaos, we explore the maximal Lyapunov exponent<sup>36–39</sup> for the evolution of the HGT stationary solution. According to refs 44–47 the maximal Lyapunov exponent is computed by

$$\lambda = \lim_{r \rightarrow 0} \lim_{t \rightarrow \infty} \frac{1}{t} \ln \frac{d(q_1, q_2; t)}{d(q_1, q_2; 0)}, \quad (5)$$

where  $d(q_1, q_2; t) = \left[ \int_{-\infty}^{\infty} |q_1(x, t) - q_2(x, t)|^2 dx \right]^{1/2}$ , which is the distance between two functions  $q_1(x, t)$  and  $q_2(x, t)$  in the Hilbert space (the  $L^2$  norm in the Hilbert space), the two initial values  $q_1(x, 0) = u_N(x)$  and  $q_2(x, 0) = u_N(x) + r(x)$ , and  $r(x)$  is a random perturbation function (as small as machine precision allows, e.g., in the order of  $10^{-8}$ ).

For a partial differential equation, the Lyapunov spectrum (all the Lyapunov exponents sorted decreasingly) converges to a smooth curve, although the number of Lyapunov exponents is dependent on the number of discretization  $M$ <sup>46</sup>. In our numerical calculations, we choose  $M=2048, 4096, 8192$ , each of them with the window size  $L=40, 50, 60$ . We find that the statistical errors of the maximal Lyapunov exponents for every initial input are less than 10% (the maximal Lyapunov exponents are nearly independent on  $r(x)$  or the renormalization step-size).

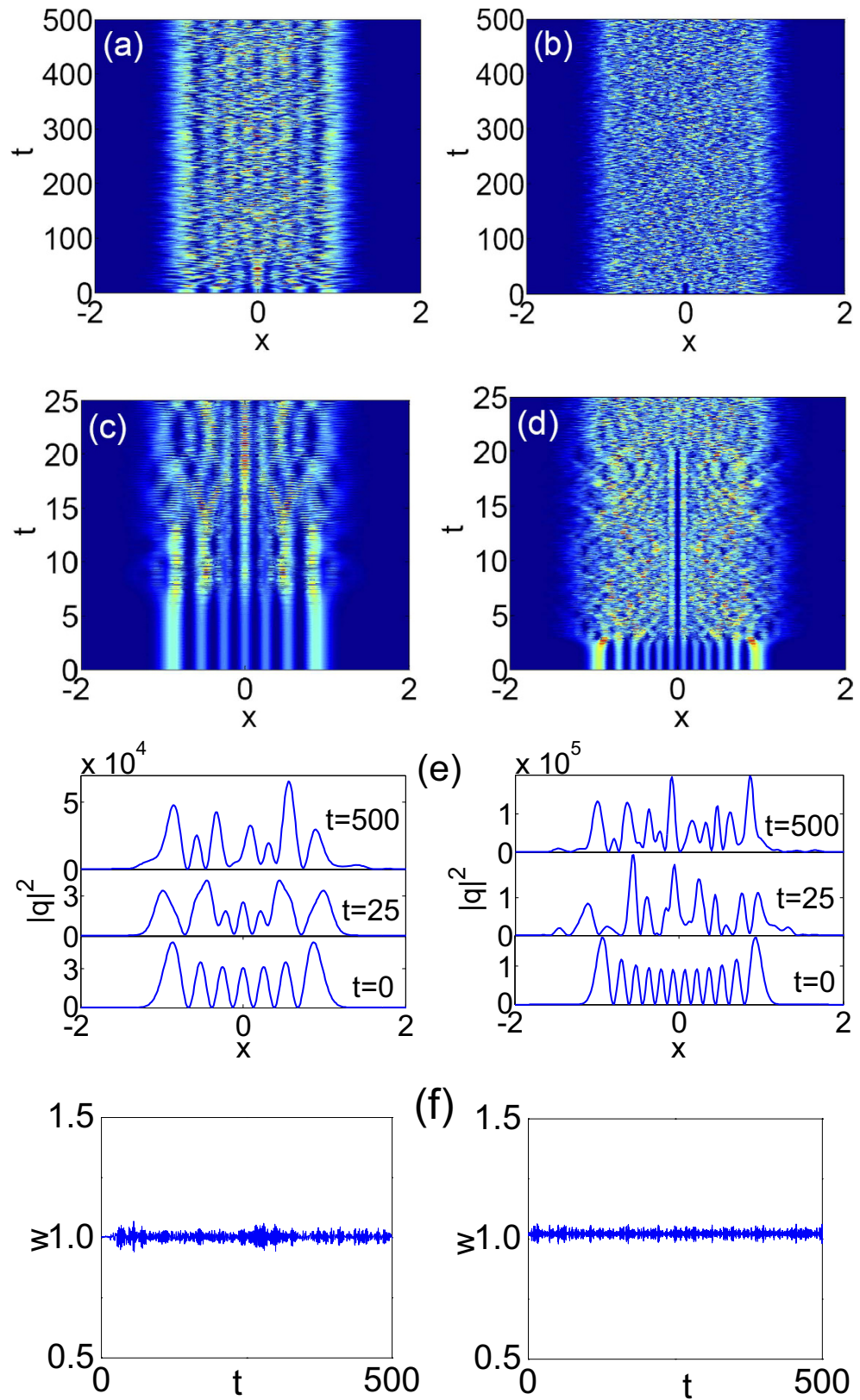


**Figure 1.** The unstable evolutions of the NNLSE for the initial inputs of the HGT stationary solutions. (a,b) The contour plots for the intensity  $|q(x, t)|^2$ , (c,d) the enlargement of the initial region of  $[0, 25]$  in (a,b), (e) profiles of the intensity at different  $t$ , (f) the statistic width  $w$ . The left and right columns are for the stationary solutions with  $N=7$  and 12, respectively.

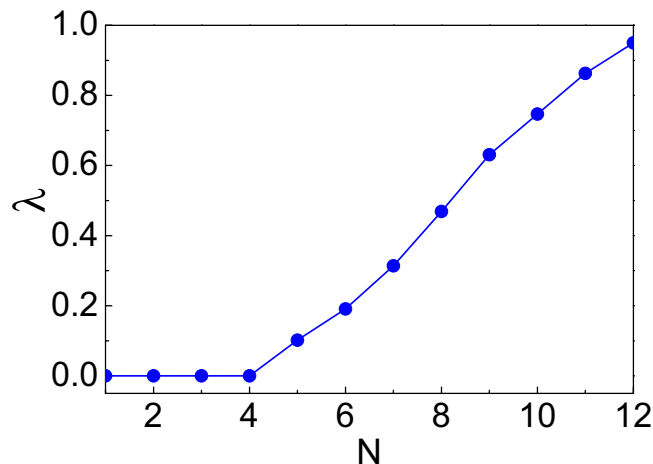


**Figure 2.** The maximal Lyapunov exponents for the evolution of the HGT stationary solutions with different  $N$ . They are average values obtained by choosing the number of discretization  $M = 2048, 4096, 8192$ , each of them with the window size  $L = 40, 50, 60$ .

Then we get the average values of the maximal Lyapunov exponents for the HGT stationary solutions with  $N \leq 12$ , as summarized in Fig. 2. We can see obviously that the maximal Lyapunov exponents for the unstable stationary solutions are all positive and increase monotonously with  $N$ , while those for solitons are equal to zero. The occurrence of chaos can be understood as a consequence of the complex interactions among humps. The more humps the profile possesses, the more complex the interactions are, which leads to a higher degree of the chaos.

It is especially important to make clear that the chaotic phenomenon described above is due to the intrinsic nature of the system but not numerically induced chaos<sup>48</sup>. Although the numerical method applied is not symplectic, it has been demonstrated that this is not the relevant issue for an infinite dimensional Hamiltonian system<sup>45,49</sup>. We have confirmed numerically that the scaling property of the maximal Lyapunov exponents match the transformation invariance of Eq. (1)<sup>17</sup>. The maximal Lyapunov exponents for the HGT stationary solutions with a given number of humps under the condition of  $\tilde{w} = w/k$  ( $k$  is a positive constant) and  $\tilde{w}_m = w_m/k$  satisfy  $\tilde{\lambda} = k^2 \lambda$  within the error range allowed. The satisfaction of the scaling property is a stringent test for the reliability of numerical computations<sup>45</sup>.

Next, we will prove that the maximal Lyapunov exponents coincide with the growth rates of the initial numerical errors. Although, literally, the maximal Lyapunov exponent measures the typical exponential rate of growth of an infinitesimal perturbation, the growth of a noninfinitesimal deviation is usually well described in this way. The numerical error of the HGT stationary solutions computed by the Newton iteration method in double precision is assumed to be of the order of  $10^{-9}$ . It will make sense that the regular profiles of the initial HGT stationary solutions will be considered to become completely irregular once the deviation reaches the order of 1. We can, therefore, estimate  $t_c$  (the critical time of becoming completely irregular) by  $10^{-9} e^{\lambda t_c} = 1$ , thus obtain  $t_c \approx 20.7/\lambda$ , as shown in Fig. 3(a). From the other aspect, the process of turning to be irregular for the profiles can also be revealed directly in the evolution. Let's consider the skewness (or the third-order central-moment) of the intensity

$$s(t) = \frac{1}{P} \int_{-\infty}^{\infty} [x - x_c(t)]^3 |q(x, t)|^2 dx. \quad (6)$$

Obviously, there is  $s(0) = 0$ , since  $|u_N(x)|^2$  is symmetric. Figure 3(b) shows the evolution of  $s$  for the HGT stationary solutions with  $N = 7$  and  $12$  in the time interval  $[0, 100]$  and  $[0, 50]$ , respectively. It can be seen that  $|s|$  starts from the close neighbour of zero and then rises abruptly around a certain  $t_{cs}$ , which is defined as  $\int_0^{t_{cs}} |s(t)| dt = 0.05$ . To a great degree, the boom of the skewness indicates the complete irregularity of the intensity profiles. That is to say,  $t_{cs}$  represents the critical time of becoming completely irregular attained from the direct statistic method. The comparison between  $t_c$  and  $t_{cs}$  is given in Fig. 3(a). It is evident that the two curves always stay close to each other, which suggests that the critical times evaluated from the above two approaches agree approximately. Then we are certain that the maximal Lyapunov exponents obtained indeed indicate the exponential growth rates of perturbation.

In addition, it is expected that the spatial patterns will be spatially decorrelated in a system described by a partial-differential evolution equation with temporally chaotic behavior<sup>50–53</sup>. Then we calculate the spatial cross correlation function of two long enough wave-amplitude series at locations  $\xi$  and  $\eta$

$$c(\xi, \eta) = \lim_{T \rightarrow \infty} \frac{\int_{t_0}^T q(\xi, t) q^*(\eta, t) dt}{\sqrt{\int_{t_0}^T |q(\xi, t)|^2 dt \int_{t_0}^T |q(\eta, t)|^2 dt}}, \quad (t_0 \geq t_c), \quad (7)$$

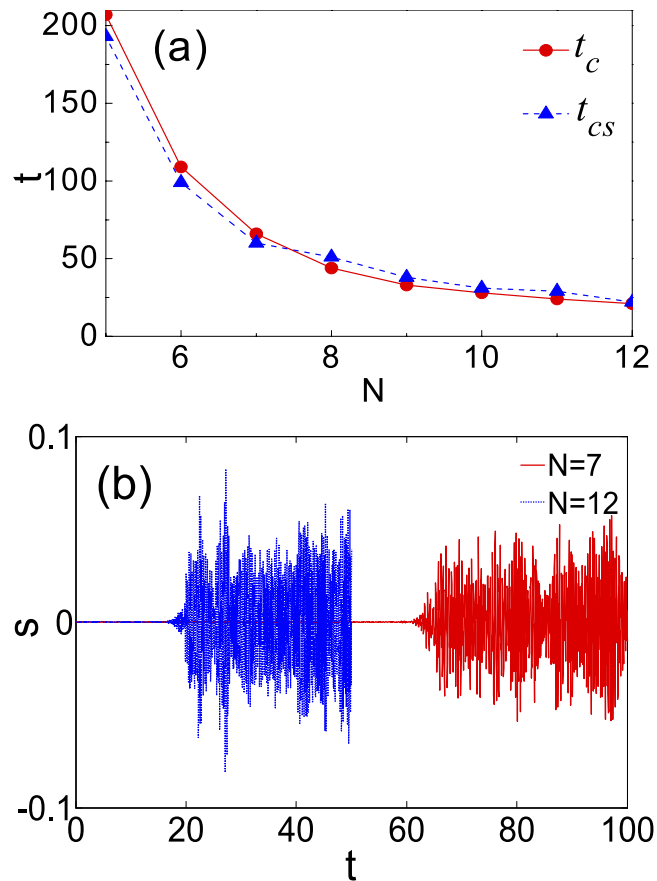


**Figure 3.** The critical times of becoming completely irregular (a) and the evolution of the skewness (b) for the unstable HGT stationary solutions.

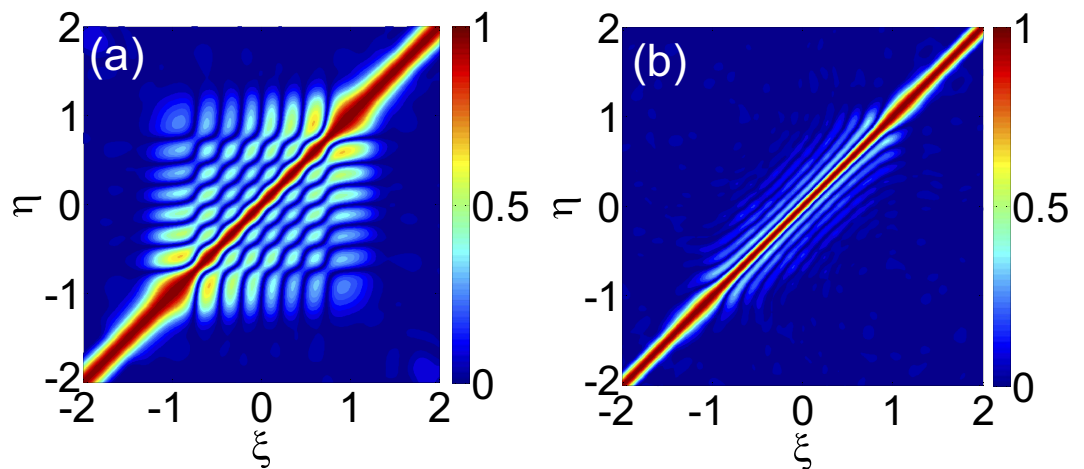


**Figure 4.** The contour plots of the spatial cross correlation functions for the HGT stationary solutions with  $N=7$  (a) and 12 (b).

where the superscript  $*$  denotes the conjugate complex. The modulus of  $c$  for the HGT stationary solutions are depicted in Fig. 4, from which we can see that  $|c|$  equals 1 along the line  $\xi = \eta$  and decreases rapidly with the separation of two locations. The quick drop of correlation in the  $x$  direction means the spatial decoherence<sup>52,53</sup>.

#### Soliton-like property I: invariant statistic width

Chaotic as they are, the evolution of the unstable HGT stationary solutions maintain almost invariant statistic width  $w$ , as shown in Fig. 1(f). The standard deviation of  $w$  during the evolution of every HGT stationary solution is less than 0.02. It is well-known that<sup>1,7,9</sup> one of two intrinsic properties for the soliton is its invariant diameter



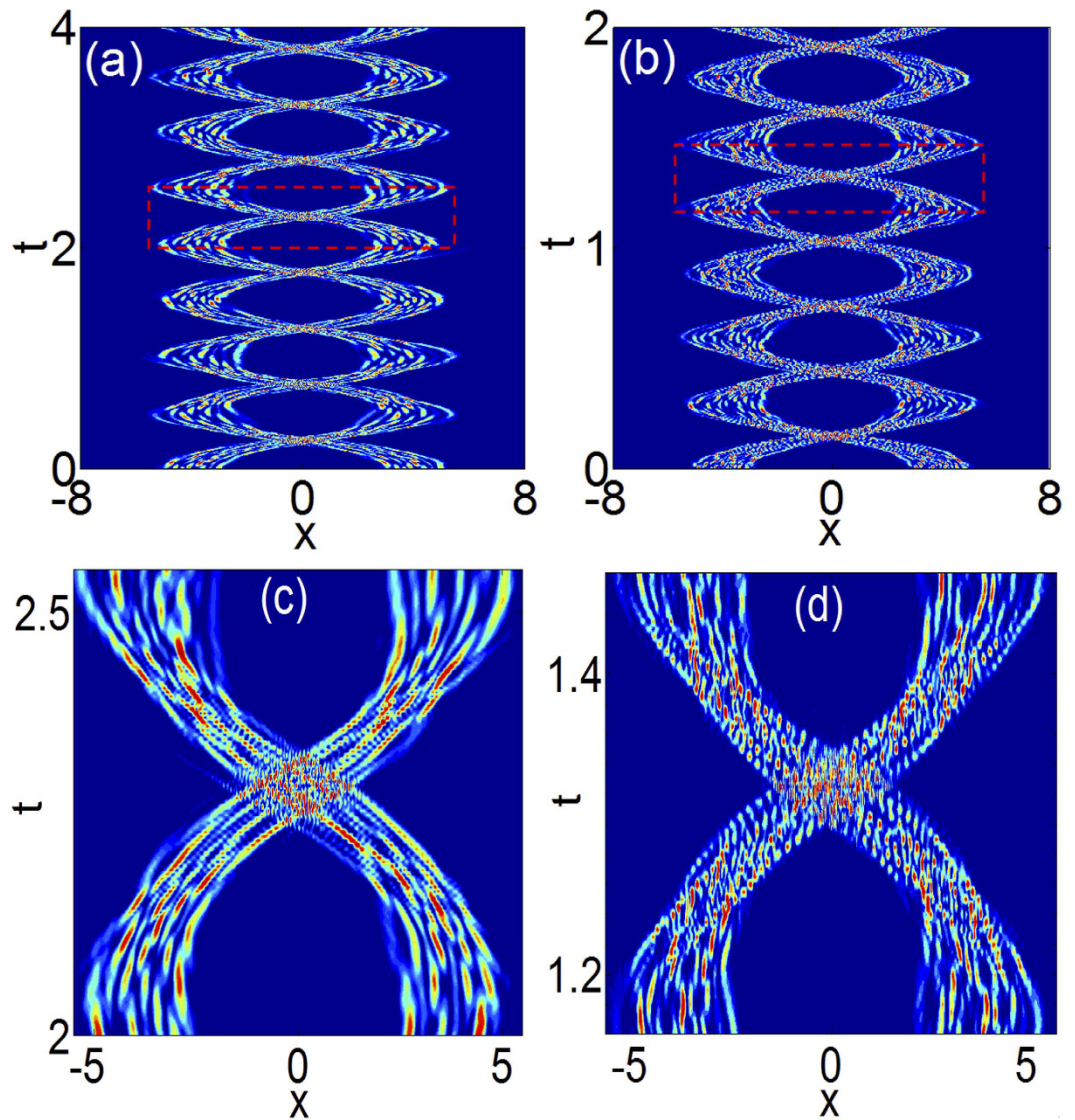


**Figure 5.** The contour plots of the intensity during the interaction of quasi-elastic collisions between the two chaoticons that are initially identical and paralleled. (a)  $N = 7$ , (b)  $N = 12$ , (c,d) partial enlarged details of (a,b) in boxes.

(width), thus we can conclude that the dynamic evolutions of the unstable HGT stationary solutions with invariant statistic widths are of such a soliton-property from the statistic point of view, even though their profiles during the evolutions are not constant. We can also see, as discussed next immediately, that they still possess the other soliton-property: a particle-like interaction. Because there co-exist the chaotic property and the soliton-like property during the dynamic evolution of the unstable HGT stationary solutions, we refer to them as chaoticons. Although we are not first to use the term “chaoticon”, the intension in both mathematics and physics of the chaoticon here is completely different from that for the spatiotemporal chaotic localized structures in dissipative systems<sup>39,40</sup>.

### Soliton-like property II: interaction of quasi-elastic collisions

Amongst all soliton properties, the important fascinating one is the particle-like interaction<sup>7,8,23</sup>. In order to check whether the chaoticons have such a property, we explore the interaction of two chaoticons that are initially identical and paralleled, which is presented in Fig. 5. The initial separation between chaoticons is large enough (8 times larger than  $w$ ) to prevent the overlap of waves, and for each case of different  $N$ s, both of the initial chaoticons are  $q(x, t_0)$  for  $t_0 \geq t_c$ , which means that the inputs are completely irregular states. We can observe that the two chaoticons attract each other, and then combine and separate quasi-periodically, much like elastic collisions between two particles. In fact, they will eventually fuse together accompanied by small energy loss to radiation after a much longer evolution. Hence, strictly speaking, the interaction is quasi-elastic.

## Some remarks

Firstly, it is worth underlining that the evolution of the unstable stationary solutions in generally or weakly non-local nonlinearity<sup>13</sup> is entirely different from those in strongly nonlocal nonlinearity discussed above. In relatively weak nonlocality, the unstable HGT stationary solution will break up and form a set of single-hump profiles by emitting remnants of their energy, which is an unbounded state since the radiation waves arrive to infinity<sup>27</sup>. We have also found that a time when the wave begin to break up increases exponentially with  $w_m$  for every HGT stationary solution with a given  $w$ . It means that the HGT stationary solutions in stronger nonlocality will evolve longer before they break up. Therefore, the radiation waves are believed to be absent in a strongly nonlocal nonlinear case<sup>27,28</sup>. Secondly, although the system considered is the  $(1 + 1)$ -dimensional NNLSE with the exponential-decay response function, our work may be readily extended to systems with different response functions<sup>21</sup> or even higher dimensions<sup>26</sup>. Thirdly, the mechanism that supports the localized spatiotemporal chaos in our conservative system is still an open problem, while the existence of dissipative chaoticons is explained analytically as the pinning and interaction of the fronts<sup>40</sup>.

## Conclusions

We have found that the unstable evolution of the  $(1 + 1)$ -dimensional NNLSE with the exponential-decay response function for the initial inputs of the HGT stationary solutions will evolve into a new kind of chaoticon, which occur only in the case of strongly nonlocal nonlinearity. The chaoticon exhibits both chaotic and soliton-like properties. The chaotic behavior is signified by the positive maximal Lyapunov exponents and spatial decoherence. The soliton-like property is demonstrated by the invariant statistic width during the evolution, as well as the quasi-elastic collisions during the interaction.

## References

1. P. G. Drazin & R. S. Johnson. *Solitons: an introduction* (2nd ed.) (Cambridge University Press, 1989).
2. M. Remoissenet. *Waves Called Solitons: Concepts and Experiments* (3rd ed.) (Springer, 1999).
3. M. Dunajski. *Solitons, Instantons, and Twistors* (Oxford University Press, 2010).
4. Y. S. Kivshar & G. P. Agrawal. *Optical Solitons: From Fibers to Photonic Crystals* (New York: Academic Press, 2003).
5. G. P. Agrawal. *Nonlinear Fiber Optics* (4th ed.) (New York: Academic Press, pp. 120–176, 2007).
6. S. Trillo & W. Torruellas. *Spatial Solitons* (Berlin: Springer, 2001).
7. G. I. Stegeman & M. Segev. Optical spatial solitons and their interactions: universality and diversity. *Science* **286**, 1518 (1999); M. Segev. Optical spatial solitons. *Opt. Quant. Electron.* **30**, 503 (1998).
8. G. I. Stegeman, D. N. Christodoulides & M. Segev. Optical spatial solitons: historical perspectives. *IEEE J. Sel. Top. Quant.* **6**, 1419 (2000).
9. Z. Chen, M. Segev & D. N. Christodoulides. Optical spatial solitons: historical overview and recent advances. *Rep. Prog. Phys.* **75**, 086401 (2012).
10. G. Assanto. *Nematicons: Spatial Optical Solitons in Nematic Liquid Crystals* (New Jersey: John Wiley & Sons, 2013).
11. Q. Guo, D. Lu & D. Deng. Nonlocal spatial optical solitons. in: X. Chen, Q. Guo, W. She, H. Zhang & G. Zhang (Eds) *Advances in Nonlinear Optics* (Berlin: De Gruyter, pp. 227–305, 2015).
12. A. W. Snyder & D. J. Mitchell. Accessible solitons. *Science* **276**, 1538 (1997).
13. W. Krolikowski, O. Bang, W. Krolikowski, J. J. Rasmussen & J. Wyller. Modulational instability in nonlocal nonlinear Kerr media. *Phys. Rev. E* **64**, 016612 (2001).
14. O. Bang, W. Krolikowski, J. Wyller & J. J. Rasmussen. Collapse arrest and soliton stabilization in nonlocal nonlinear media. *Phys. Rev. E* **66**, 046619 (2002).
15. C. Conti, M. Peccianti & G. Assanto. Route to nonlocality and observation of accessible solitons. *Phys. Rev. Lett.* **91**, 073901 (2003).
16. C. Conti, M. Peccianti & G. Assanto. Observation of optical spatial solitons in a highly nonlocal medium. *Phys. Rev. Lett.* **92**, 113902 (2004).
17. S. Ouyang, Q. Guo & W. Hu. Perturbative analysis of generally nonlocal spatial optical solitons. *Phys. Rev. E* **74**, 036622 (2006).
18. D. Deng, X. Zhao, Q. Guo & S. Lan. Hermite-Gaussian breathers and solitons in strongly nonlocal nonlinear media. *J. Opt. Soc. Am. B* **24**, 2537 (2007).
19. D. Buccoliero, A. S. Desyatnikov, W. Krolikowski & Y. S. Kivshar. Laguerre and Hermite soliton clusters in nonlocal nonlinear media. *Phys. Rev. Lett.* **98**, 053901 (2007).
20. Z. Xu, Y. V. Kartashov & L. Torner. Upper threshold for stability of multipole-mode solitons in nonlocal nonlinear media. *Opt. Lett.* **30**, 3171 (2005).
21. L. Dong & F. Ye. Stability of multipole-mode solitons in thermal nonlinear media. *Phys. Rev. A* **81**, 013815 (2010).
22. P. D. Rasmussen, O. Bang & W. Krolikowski. Theory of nonlocal soliton interaction in nematic liquid crystals. *Phys. Rev. E* **72**, 066611 (2005).
23. C. Rotschild, B. Alfassi, O. Cohen & M. Segev. Long-range interactions between optical solitons. *Nat. Phys.* **2**, 769 (2006).
24. S. Ouyang, W. Hu & Q. Guo. Light steering in a strongly nonlocal nonlinear medium. *Phys. Rev. A* **76**, 053832 (2007).
25. W. Hu, S. Ouyang, P. Yang, Q. Guo & S. Lan. Short-range interactions between strongly nonlocal spatial solitons. *Phys. Rev. A* **77**, 033842 (2008).
26. S. Skupin, O. Bang, D. Edmundson & W. Krolikowski. Stability of two-dimensional spatial solitons in nonlocal nonlinear media. *Phys. Rev. E* **73**, 066603 (2006).
27. I. Kaminer, C. Rotschild, O. Manela & M. Segev. Periodic solitons in nonlocal nonlinear media. *Opt. Lett.* **32**, 3209 (2007).
28. C. Rotschild, T. Schwartz, O. Cohen & M. Segev. Incoherent spatial solitons in effectively instantaneous nonlinear media. *Nat. Photon.* **2**, 371 (2008).
29. A. Picozzi & J. Garnier. Incoherent soliton turbulence in nonlocal nonlinear media. *Phys. Rev. Lett.* **107**, 233901 (2011).
30. W. Hong, Q. Guo & L. Li. Dynamics of optical pulses in highly noninstantaneous Kerr media. *Phys. Rev. A* **92**, 023803 (2015).
31. F. Dalfovo, S. Giorgini, L. Pitaevskii & S. Stringari. Theory of Bose-Einstein condensation in trapped gases. *Rev. Mod. Phys.* **71**, 463 (1999).
32. T. Lahaye, C. Menotti, L. Santos, M. Lewenstein & T. Pfau. The physics of dipolar bosonic quantum gases. *Rep. Prog. Phys.* **72**, 126401 (2009).
33. S. Skupin, M. Saffman & W. Krolikowski. Nonlocal stabilization of nonlinear beams in a self-focusing atomic vapor. *Phys. Rev. Lett.* **98**, 263902 (2007).
34. C. Rotschild, O. Cohen, O. Manela & M. Segev. Solitons in nonlinear media with an infinite range of nonlocality: first observation of coherent elliptic solitons and of vortex-ring solitons. *Phys. Rev. Lett.* **95**, 213904 (2005).
35. Q. Guo, W. Hu, D. Deng, D. Lu & S. Ouyang. Features of strongly nonlocal spatial solitons. In: G. Assanto (Ed.), *Nematicons: Spatial Optical Solitons in Nematic Liquid Crystals* (New Jersey: John Wiley & Sons, pp. 37–69, 2013).

36. J. C. Sprott. *Chaos and Time-Series Analysis* (Oxford University Press, 2003).
37. H. G. Schuster & W. Just. *Deterministic Chaos: An Introduction* (Weinheim: Wiley-VCH Verlag GmbH & Co. KGaA, 2005).
38. J. J. Lissauer. Chaotic motion in the solar system. *Rev. Mod. Phys.* **71**, 835 (1999).
39. N. Verschuere, U. Bortolozzo, M. G. Clerc & S. Residori. Spatiotemporal chaotic localized state in liquid crystal light valve experiments with optical feedback. *Phys. Rev. Lett.* **110**, 104101 (2013)
40. N. Verschuere, U. Bortolozzo, M. G. Clerc & S. Residori. Chaoticon: localized pattern with permanent dynamics. *Phil. Trans. R. Soc. A* **372**, 0011 (2014).
41. L. Zhong, J. Yang, Z. Ren & Q. Guo. Hermite-Gaussian stationary solutions in strongly nonlocal nonlinear optical media. *Opt. Commun.* **383**, 274 (2017).
42. A. C. Yew, A. R. Champneys & P. J. McKenna. Multiple solitary waves due to second-harmonic generation in quadratic media. *J. Nonlinear Sci.* **9**, 33 (1999).
43. G. P. Agrawal. *Nonlinear Fiber Optics* (4th ed.) (New York: Academic Press, p. 41, 2007).
44. A. C. Cassidy, D. Mason, V. Dunjko & M. Olshanii. Threshold for chaos and thermalization in the one-dimensional mean-field Bose-Hubbard model. *Phys. Rev. Lett.* **102**, 025302 (2009).
45. I. Brezinova, L. A. Collins, K. Ludwig, B. I. Schneider & J. Burgdorfer. Wave chaos in the nonequilibrium dynamics of the Gross-Pitaevskii equation. *Phys. Rev. A* **83**, 043611 (2011).
46. M. G. Clerc & N. Verschuere. Quasiperiodicity route to spatiotemporal chaos in one-dimensional pattern-forming systems. *Phys. Rev. E* **88**, 052916 (2013).
47. G. Tancredi, A. Sánchez & F. Roig. A comparison between methods to compute Lyapunov exponents. *Astron. J* **121**, 1171 (2001).
48. B. M. Herbst & M. J. Ablowitz. Numerically induced chaos in the nonlinear Schrödinger equation. *Phys. Rev. Lett.* **62**, 2065 (1989); M. J. Ablowitz, C. Schober & B. M. Herbst. Numerical chaos, roundoff errors, and homoclinic manifolds. *Phys. Rev. Lett.* **71**, 2683 (1993).
49. M. J. Ablowitz, B. M. Herbst & C. M. Schober. On the numerical solution of the Sine-Gordon equation. *J. Comput. Phys.* **131**, 354 (1997); D. J. Kouri, D. Zhang, G. Wei, T. Konshak & D. K. Hoffman. Numerical solutions of nonlinear wave equations. *Phys. Rev. E* **59**, 1274 (1999).
50. M. C. Cross & P. C. Hohenberg. Spatiotemporal Chaos. *Science* **263**, 1569 (1994).
51. D. Cai & D. W. McLaughlin. Chaotic and turbulent behavior of unstable one-dimensional nonlinear dispersive waves. *J. Math. Phys.* **41**, 4125 (2000).
52. E. Shlizerman & V. Rom-Kedar. Parabolic resonance: A route to Hamiltonian spatiotemporal chaos. *Phys. Rev. Lett.* **102**, 033901 (2009).
53. R. Ramaswamy & F. Julicher. Activity induces traveling waves, vortices and spatiotemporal chaos in a model actomyosin layer. *Sci. Rep.* **6**, 20838 (2016).

## Acknowledgements

We are grateful to Prof. Senyue Lou at Ningbo University for his great help during the work. This research was supported by the National Natural Science Foundation of China, Grant Nos. 11474109 and 11675054.

## Author Contributions

Q. Guo and L. Zhong conceived and designed the study. L. Zhong carried out the numerical computation and wrote the manuscript. Y. Li and Y. Chen provided the approach of representation. W. Hong and W. Hu assisted with the numerical computation and the theoretical analysis. All authors read and approved the manuscript.

## Additional Information

**Competing financial interests:** The authors declare no competing financial interests.

**How to cite this article:** Zhong, L. *et al.* Chaoticons described by nonlocal nonlinear Schrödinger equation. *Sci. Rep.* **7**, 41438; doi: 10.1038/srep41438 (2017).

**Publisher's note:** Springer Nature remains neutral with regard to jurisdictional claims in published maps and institutional affiliations.



This work is licensed under a Creative Commons Attribution 4.0 International License. The images or other third party material in this article are included in the article's Creative Commons license, unless indicated otherwise in the credit line; if the material is not included under the Creative Commons license, users will need to obtain permission from the license holder to reproduce the material. To view a copy of this license, visit <http://creativecommons.org/licenses/by/4.0/>

© The Author(s) 2017